Reynolds averaged theory of turbulent shear flows over undulating beds and formation of sand waves

Sujit K. Bose

Centre for Theoretical Studies, Indian Institute of Technology, Kharagpur, 721302 West Bengal, India

Subhasish Dey[*]

Department of Civil Engineering, Indian Institute of Technology, Kharagpur, 721302 West Bengal, India
(Received 22 December 2008; revised manuscript received 24 June 2009; published 3 September 2009)

Based on the Reynolds averaged Navier-Stokes (RANS) equations and the time-averaged continuity equation, a theory of turbulent shear flow over an undulating sand bed is developed addressing the instability criterion of plane sand beds in free-surface flows leading to the formation of sand waves. In the analysis, the integration of RANS equations leads to generalized Saint Venant equations, in which the time-averaged streamwise velocity is characterized by a power law obtained from turbulence closure, treating the curvilinear streamlines by the Boussinesq approximation. As a consequence, the modified pressure distribution has a departure from the traditionally linear hydrostatic pressure distribution. The instability analysis of a plane sand bed yields the curves of the Froude number versus nondimensional wave number, determining an instability zone for which at lower Froude numbers (less than 0.8), the plane bed becomes unstable with the formation of dunes; whereas at higher Froude numbers, the plane bed becomes unstable with the formation of standing waves and antidunes. For higher Froude numbers, the experimental data for antidunes lie within the unstable zone; while for lower Froude numbers, the same is found for dunes with some experimental scatter.

I. INTRODUCTION

Unidirectional flow over a sand bed interacts with the sand particles to develop bedforms. Due to immense research and practical importance, the flow feature over bedforms, the formation of bedforms and their characteristics have been explored over five decades [1–4]. Anderson [5] was the first to describe the characteristics of the fully developed sand waves, assuming potential flow over a sinusoidal bed and the mode of sediment transport as bed load. Benjamin [6] studied the shear flow over rigid undulating beds to determine the normal and tangential stresses. Kennedy [7] analyzed the formation of dunes and antidunes in the context of two-dimensional stability; he also used the potential flow solution. In order to produce an unstable wave, he introduced a quantity that was defined as a spatial or phase lag between the local sediment transport rate and the local bed velocity. Nevertheless, in an earlier study, the occurrence of the phase lag between the bedform (and thus the sediment transport) and the flow velocity was also shown by Exner [8] having included the bed frictional resistance. Subsequently, Reynolds [9] enhanced Kennedy's theory by three-dimensional stability analysis, which was further studied by Engelund and Fredsøe [10], assuming a sediment transport model of suspension. Engelund and Hansen [11] developed a stability theory of flow over a sinusoidal sand bed, considering real fluid flow. They accounted for the departure in pressure distribution from the traditional hydrostatic pressure distribution due to the vertical acceleration of fluid induced by the sinusoidal bed. The stable and unstable bed conditions were determined using the phase lag distance of sediment trans-

port rate from the bed shear stress. Their model can also be applicable to study the occurrence of three-dimensional sand waves. Hayashi [12] gave an improved explanation (physical and quantitative) for the phase lag following a two-dimensional stability analysis based on potential fluid flow. Engelund [13] put forward a reasonable model of the sediment transport based on the vorticity transport equation of two-dimensional real fluid flow and a diffusion equation of sediment suspension. The model explains the phase lag between the flow rate and the sediment transport rate. Smith [14] applied the same approach but restricted to the flow of low Froude numbers. Later, Fredsøe [15] extended the work of Engelund [13] by introducing the influence of the local bed slope on the bed-load transport rate. He found that at low Froude numbers, the bed slope controls the unstable waves to low wave numbers. For the formation of ripples and dunes, Richards [16] proposed a stability theory (based on hydraulically rough regime) that predicts the occurrence of two separate modes of "instability." The instability mode with the wavelengths as a function of bed roughness corresponds to the formation of ripples, while the instability mode with the flow depth refers to the formation of dunes. A kinematic wave theory, developed by Song [17] basically for the purposes of flood routing, was generalized to account for additional coupling between kinematics and dynamics of a continuum system. Converting the continuity equation into the mass transport equation, the theory was made applicable to predict the migration speed of sand waves and the growth or decay of these waves. Onda and Hosoda [18] developed a depth-averaged flow model to reproduce the formation process of sand dunes and the flow resistance considering the effect of vertical acceleration and nonequilibrium sediment transport. The results obtained by them were well comparable with the experimental data. Besides these, some other

_____
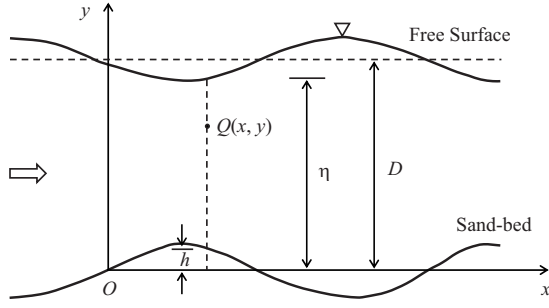*Corresponding author; sdey@iitkgp.ac.in

FIG. 1. Definition sketch of flow over an undulating sand bed.

researchers explored the bedforms in closed ducts [19–21]. Although they pointed out that the developed bedforms in closed ducts and open channels are closely related phenomena having free-surface waves in open channel as an effect rather than a cause of dune formation or its development, it is intuitive that for flow over dunes in a closed duct, the piezometric line (that is hydraulic grade line), which represents the free-surface profile in open channels, should be wavy. This issue was straightway ignored in these studies as no measurement of piezometric line in flow through ducts was done. Nevertheless, the formation of dunes in closed duct is beyond the realm of this study.

In this paper, based on the Reynolds averaged Navier-Stokes (RANS) equations and the time-averaged continuity equation, a theory of turbulent shear flow over an undulating sand bed is developed. The theory addresses the instability of a plane sand bed in free-surface flows leading to the formation of sand waves. The results obtained from the instability analysis are validated by the experimental data of various researchers.

The present theory lies on its original and systematic derivation procedure of the dynamic instability of the bedforms (in Sec. VI) following the turbulence closure (in Sec. III) and the Boussinesq flow approximation for small streamline curvatures (in Sec. IV). In the process of integration of RANS equations, a generalized Saint Venant equation is obtained (in Sec. V). All these aspects are addressed in a single theory presented here. Importantly, the results obtained on the stability of sand wave or bedforms using this theory is superior to those obtained from earlier theories (in Sec. VI) because the stable and unstable bed-forms can be separated out in a better and well-defined way.

II. RANS EQUATIONS

In Fig. 1, a unidirectional flow over a gradual undulating sand bed (slowly erodible) of small amplitude (that is the bed perturbation) is considered. The x axis considered passes through the mean bed level, and the origin O is set conveniently on this axis. The y axis is therefore vertically upwards. For an erodible sand bed, the bed elevation is a function of both horizontal distance x and time t, say $h(x,t)$, where h is the height of sand wave above a certain mean level. The bed undulation causes a wavy profile of the free surface of flow with height above the mean bed level, like-

wise a function of x and t, say $\eta(x,t)$. However, the height from the mean bed level (that is x axis) to the mean free-surface profile is assumed to be a constant D, termed mean flow depth. Due to the consideration of gradual variation in the bed undulation, the maximum amplitude $|h|$ is small compared to the horizontal length scale of the bedforms and its streamwise gradient $|\partial h/\partial x| \ll 1$. Likewise, $|\eta|$ must be small and $|\partial \eta/\partial x| \ll 1$, provided that there exists a no-choke flow. Note that the choke flow refers to the severe bed perturbation for which no physical solution of flow exists as a result of which in practice, a hydraulic jump or surge (that may travel either upstream or downstream) or backwater effect is developed.

It is pertinent to assume that the bedforms and their roughness generate turbulence in the fluid medium. Referring to the coordinate system in Fig. 1, according to Reynolds decomposition, the instantaneous velocity components (u,v) at any point $Q(x,y)$ can then be split into the time-averaged part $(\bar{u},\bar{v})$ and the fluctuating part (u',v') as

$$u(x,y,t) = \bar{u}(x,y,t) + u'(x,y,t), \quad v(x,y,t) = \bar{v}(x,y,t) + v'(x,y,t). \tag{1}$$

The continuity equations for the time-averaged velocities $(\bar{u},\bar{v})$ and their fluctuations (u',v') are

$$\frac{\partial \bar{u}}{\partial x} + \frac{\partial \bar{v}}{\partial y} = 0, \quad \frac{\partial u'}{\partial x} + \frac{\partial v'}{\partial y} = 0. \tag{2}$$

The exact RANS equations of two-dimensional turbulent flow are of the form

$$\frac{\partial \bar{u}}{\partial t} + \bar{u}\frac{\partial \bar{u}}{\partial x} + \bar{v}\frac{\partial \bar{u}}{\partial y} = -\frac{\partial \bar{P}}{\partial x} + \frac{\partial \tau}{\partial y} + v\frac{\partial^2 \bar{u}}{\partial y^2} - \frac{\partial(\overline{u'^2})}{\partial x}, \tag{3a}$$

$$\frac{\partial \bar{v}}{\partial t} + \bar{u}\frac{\partial \bar{v}}{\partial x} + \bar{v}\frac{\partial \bar{v}}{\partial y} = -\frac{\partial \bar{P}}{\partial y} + \frac{\partial \tau}{\partial x} + v\frac{\partial^2 \bar{v}}{\partial x^2} - \frac{\partial(\overline{v'^2})}{\partial y} - g, \tag{3b}$$

where $\bar{P}(x,y,t)$ is the time-averaged hydrostatic pressure relative to mass density of fluid ρ, $\tau(x,y,t)$ is $-\overline{u'v'}$, that is the Reynolds shear stress relative to ρ, v is the kinematic viscosity of fluid, and g is the acceleration due to gravity. In the above equations, the overbar of a quantity denotes the time-averaged value of the quantity. Equations (2) and (3b) form an undetermined system, since there are six dependent parameters (namely, $\bar{u}, \bar{v}, u', v', \bar{P}$, and τ) against five equations. As a result of which, additional assumptions need to be made based on the characteristics of the flow under consideration.

III. TURBULENCE CLOSURE

The turbulence is characterized by fully developed flow throughout the flow domain except possibly very close to the bed, where the velocity tends to be zero following a thin viscous layer. In addition, the flow is essentially described by a turbulent shear flow, devoid of excessive agitated heaving

of the free surface. For such conditions, the gradients of the Reynolds stresses along the streamwise direction are nearly zero. Thus, one obtains the primary features on turbulence as follows:

$$\frac{\partial \tau}{\partial x} \approx 0, \quad \frac{\partial (\overline{u'^2})}{\partial x} \approx 0, \quad \frac{\partial (\overline{v'^2})}{\partial x} \approx 0. \tag{4}$$

The above relationships are indeed exact in streamwise flow over a plane bed. Nevertheless, they are legitimate for the wavy beds having gradual bed profile variation in the streamwise direction.

The second postulation is on the law of variation in streamwise velocity $\bar{u}$ with y in turbulent flow. When the bed is a plane horizontal, a layered model for $\bar{u}$ is commonly used, in which a thin viscous layer is overlain by a buffer layer (transitional layer), a turbulent layer defined by logarithmic law and a top turbulent outer layer (wake layer). However, to make a substantive progress in the analysis, a single averaged distribution of $\bar{u}$ is considered following the $1/p$th power law of depth y introduced by Schlichting [22], where p is usually taken as 7 for the turbulent flow over a rigid boundary [23]. The primary advantage of considering power law, which is a slowly varying function of y as is the logarithmic law, is that the integration of the RANS equations can be obtained explicitly (see Sec. V). On the other hand, by using logarithmic law, explicit equations from the integration of the RANS equations cannot be obtained. Thus, one can write

$$\bar{u} = U_0(x,t) \left(\frac{y-h}{\eta - h} \right)^{1/p}, \tag{5}$$

where U_0 is the maximum velocity at $y = \eta$. An advantage of using this form is that $\bar{u} \to 0$ as $y \to h$, allowing one to ignore the consideration of viscous layer close to the bed.

A theoretical justification of the approximation by the power law [Eq. (5)] may be sought as in Bose and Dey [24,25]. It is based on the fact that in the streamwise and vertical directions, the turbulent stresses $|\partial \tau / \partial y|$ and $|\partial \tau / \partial x|$ dominate the respective viscous stresses $|v \partial^2 \bar{u} / \partial y^2|$ and $|v \partial^2 \bar{v} / \partial x^2|$ in the momentum [Eqs. (3a) and (3b))] varying slowly with the vertical distance y. The nature of the variation with y is concluded from that of inviscid flow, inasmuch as the variation must be absent. Thus, one can propose

$$\left| v \frac{\partial^2 \bar{u}}{\partial y^2} \right| \ll \left| \frac{\partial \tau}{\partial y} \right| \quad \text{and} \quad \left| v \frac{\partial^2 \bar{v}}{\partial x^2} \right| \ll \left| \frac{\partial \tau}{\partial x} \right| \approx 0 \tag{6}$$

for a slowly varying variable in the vertical direction above the undulating bed, say $\zeta = (y-h)^{1/p}$, where $p > 1$. Since $y - h = \zeta^p$ and $dy = p\zeta^{p-1} d\zeta$, the first condition in Eq. (6) becomes

$$\left| \frac{\partial^2 \bar{u}}{\partial \zeta^2} \right| \ll \frac{p \zeta^{p-1}}{v} \left| \frac{\partial \tau}{\partial \zeta} \right| \tag{7}$$

so that in the turbulent zone $\zeta \ge \delta$, where δ is a small positive constant, one can write

$$\left| \frac{\partial^2 \bar{u}}{\partial \zeta^2} \right| \le \varepsilon \ll \frac{p \delta^{p-1}}{v} \min \left\{ \left| \frac{\partial \tau}{\partial \zeta} \right| \right\}, \tag{8}$$

where $\varepsilon > 0$ defines the actual maximum value of the second derivative of $\bar{u}$ in magnitude. It is much less than the right-hand side of Eq. (8). The left-hand side of inequality (8) implies that $-\varepsilon \le \partial^2 \bar{u} / \partial \zeta^2 \le \varepsilon$, whose appropriate solution is

$$\bar{u} = A(x,t) + B(x,t)\zeta + \theta \varepsilon \zeta^2 \quad \text{with} \quad \zeta \ge \delta \quad \text{and} \quad -0.5 \le \theta$$
$$\le 0.5, \tag{9}$$

where θ is an uncertainty function. As $\bar{u} \to 0$ for $\zeta \to 0$, $A(x,t) = 0$. Setting $B(x,t) = U_0(x,t)/(\eta - h)^{1/p}$ and dropping the uncertain small term containing $\theta \varepsilon$, one obtains $\bar{u}$ in the form of Eq. (5). It is assumed that the form can be continued for $\zeta \to 0$ or $y \to h$.

In Eq. (5), the term U_0 represents the maximum velocity at a flow section. It can be related to the depth-averaged velocity $U(x,t)$ at that flow section as

$$U(x,t) = \frac{1}{\eta - h} \int_h^\eta \bar{u} \, dy = \frac{p}{1+p} U_0(x,t). \tag{10}$$

Hence, using Eq. (10), Eq. (5) can be written in terms of U as

$$\bar{u} = \frac{1+p}{p} U(x,t) \left(\frac{y-h}{\eta - h} \right)^{1/p}. \tag{11}$$

The continuity Eq. (2), then approximately yields

$$\bar{v} = -(\eta - h) \frac{\partial U}{\partial x} \left(\frac{y-h}{\eta - h} \right)^{(1+p)/p}. \tag{12}$$

The velocity distribution is thus expressed in terms of depth-averaged velocity U, taking into account $1/p$th power law variation in $\bar{u}$ with height.

IV. FLOW CHARACTERISTICS

The streamwise free-surface profile over a gradual undulating bed possesses a curvature with insignificant streamwise gradient. It implies that as $|\partial h/\partial x| \approx 0$, $|\partial \eta/\partial x| \approx 0$. Moreover, in the motion along a streamline having a small curvature, the normal acceleration is considered to be essentially advective for vanishing local acceleration that is $\partial \bar{v}/\partial t \approx 0$ due to the small magnitude of rise and fall of a fluid element. By Eq. (2), the advective vertical acceleration is given by

$$\bar{u} \frac{\partial \bar{v}}{\partial x} + \bar{v} \frac{\partial \bar{v}}{\partial y} = \bar{u} \frac{\partial \bar{v}}{\partial x} - \bar{v} \frac{\partial \bar{u}}{\partial x} = \bar{u}^2 \frac{\partial (\tan \psi)}{\partial x} \approx \bar{u}^2 \kappa, \tag{13}$$

where $\tan \psi$ is the slope of a streamline through the point $Q(x,y)(=\bar{v}/\bar{u})$ and κ is the curvature of the streamline through the point Q, such that $\kappa(h) \approx \partial^2 h/\partial x^2$ and $\kappa(\eta) \approx \partial^2 \eta/\partial x^2$, in which the slopes are negligible. Following the Boussinesq theory, one can use a linear variation in κ between the curvatures $\kappa(h)$ and $\kappa(\eta)$ at levels h and η (that is $h \le y \le \eta$), respectively, so that

$$\kappa = \kappa(h) + [\kappa(\eta) - \kappa(h)]\frac{y-h}{\eta-h}. \qquad (14)$$

With this value of κ in Eq. (13) and $\bar{u}$ given by Eq. (5), Eq. (3b) is integrated with respect to y and the resulting equation is

$$\bar{P} = \bar{P}_0 + g(\eta-y) - U^2(\eta-h)\left(\frac{1+p}{p}\right)^2\left\{\frac{p}{2+p}\kappa(h)\right.$$

$$\times\left[\left(\frac{y-h}{\eta-h}\right)^{(2+p)/p} - 1\right] + \frac{p}{2(p+1)}[\kappa(\eta)-\kappa(h)]$$

$$\left.\times\left[\left(\frac{y-h}{\eta-h}\right)^{2(1+p)/p} - 1\right]\right\} - \overline{v'^2}, \qquad (15)$$

where $\bar{P}_0$ is the value of $\bar{P}$ at $y=\eta$. The above equation yields $\partial\bar{P}/\partial x$, noting that the contribution of $\overline{v'^2}$ is negligible due to negligible variations of turbulence stresses, as given in Eq. (4). The gravity curvature of flow and $1/p$th power law of variation in streamwise velocity with height contribute to the expression for $\partial\bar{P}/\partial x$. The expression for $\partial\bar{P}/\partial x$ is used in the momentum Eq. (3a).

V. INTEGRATION OF RANS EQUATIONS

Assuming an infinite theoretical stretch of fluid in the horizontal direction, the fluid zone is assumed as if it were a thin layer spread over a bed, in which flow velocity is convenient to be expressed in terms of depth-averaged velocity U. Integration the continuity Eq. (2) and using Eq. (10), one can write

$$\frac{D\eta}{Dt} - \frac{Dh}{Dt} = \bar{v}|_h^\eta = -\int_h^\eta \frac{\partial\bar{u}}{\partial x}dy = -\frac{\partial}{\partial x}[(\eta-h)U]$$

$$+ \bar{u}(x,\eta,t)\frac{\partial\eta}{\partial x} - \bar{u}(x,h,t)\frac{\partial h}{\partial x}. \qquad (16)$$

In the above, $D(\cdot)/Dt$ denotes the total (local and advective) time derivative $\partial(\cdot)/\partial t + \bar{u}\partial(\cdot)/\partial x$. The above equation thus reduces to

$$\frac{\partial}{\partial t}(\eta-h) + \frac{\partial}{\partial x}[(\eta-h)U] = 0. \qquad (17)$$

For integrating Eq. (3a), from Eq. (15) one gets

$$\int_h^\eta \frac{\partial\bar{P}}{\partial x}dy = g(\eta-h)\frac{\partial\eta}{\partial x} + \gamma\frac{\partial}{\partial x}\left\{U^2(\eta-h)^2\left[\kappa(\eta)\right.\right.$$

$$\left.\left.+ \frac{p}{2(p+1)}\kappa(h)\right]\right\}, \qquad (18)$$

where $\gamma = (p+1)^2/[p(3p+2)]$. Similarly, for the advective acceleration by partially integrating the third term of the left-hand side of Eq. (3a) using Eqs. (2) and (11), one gets

$$\int_h^\eta\left(\frac{\partial\bar{u}}{\partial t} + \bar{u}\frac{\partial\bar{u}}{\partial x} + \bar{v}\frac{\partial\bar{u}}{\partial y}\right)dy = \frac{\partial}{\partial t}[(\eta-h)U] + \frac{\partial}{\partial x}\int_h^\eta \bar{u}^2 dy$$

$$= \frac{\partial}{\partial t}[(\eta-h)U] + \sigma\frac{\partial}{\partial x}[(\eta-h)U^2], \qquad (19)$$

where $\sigma = (p+1)^2/[p(p+2)]$. Applying the conditions of Eq. (4), the integration of Eq. (3a) with respect to y yields

$$\frac{\partial}{\partial t}[(\eta-h)U] + \sigma\frac{\partial}{\partial x}[(\eta-h)U^2] + \gamma\frac{\partial}{\partial x}\left\{(\eta-h)^2U^2\left[\kappa(\eta)\right.\right.$$

$$\left.\left.+ \frac{p}{2(p+1)}\kappa(h)\right]\right\} + g(\eta-h)\frac{\partial\eta}{\partial x} + gn^2\frac{U^2}{(\eta-h)^{1/3}} = 0, \qquad (20)$$

where n is the Manning roughness coefficient for the skin frictional resistance on the surface of undulating sand beds. In the above derivation, the Reynolds stress $\tau(y)$ essentially vanishes at both $y=h$ and η. On the other hand, the viscous shear stress $\upsilon\rho\partial\bar{u}/\partial y$ is not accurately described by the representation of $\bar{u}$ in Eq. (5). Alternatively, the viscous shear stress is negligible near the free surface $y=\eta$ as the profile of $\bar{u}$ is nearly vertical, while at the bed ($y=h$), it equals bed shear stress τ_0. The latter is represented in Eq. (20) by applying the Manning equation locally for estimation of skin frictional resistance as $\rho u_\tau^2 = \tau_0 = \rho gn^2U^2/(\eta-h)^{1/3}$; where u_τ is the shear velocity at distance x. Apparently this expression can be the leading term of an expression containing possibly additional very small contributions from the very small slope (less than 0.1 upstream slope of a dune) and the curvature of the bed. Such contributions do not alter the investigation of sand waves studied in Sec. VI when the linearization of the equations has been affected. Retaining the principal term as in the foregoing, the expression of τ_0 corresponds to its maximum and minimum values near the crest and the trough of a bedform, respectively. This follows from the fact that the free-surface profile of η exhibits a spatial phase lag of the crest of the free-surface profile with respect to that of the sand wave of h. This implies a reduction in $\eta-h$ near a sand-bed crest and consequent increase in velocity U. The reverse phenomenon takes place near a sand-bed trough. Performing the differentiations of Eq. (20), one can obtain an alternative form of Eq. (20) as

$$\frac{\partial U}{\partial t} + (2\sigma-1)U\frac{\partial U}{\partial x} + (\sigma-1)\frac{U^2}{\eta-h}\frac{\partial}{\partial x}(\eta-h) + \gamma(\eta$$

$$-h)U^2\left[\frac{\partial\kappa(\eta)}{\partial x} + \frac{p}{2(p+1)}\frac{\partial\kappa(h)}{\partial x}\right] + 2\gamma U\left[\kappa(\eta)\right.$$

$$\left.+ \frac{p}{2(p+1)}\kappa(h)\right]\frac{\partial}{\partial x}[(\eta-h)U] + g\frac{\partial\eta}{\partial x} + gn^2\frac{U^2}{(\eta-h)^{4/3}}$$

$$= 0. \qquad (21)$$

Equation (20) or Eq. (21) may be viewed as a generalization of the Saint Venant equation, in which the variability of $\bar{u}$ according to $1/p$th power law and the curvature of streamlines are taken into consideration.

For application of Eq. (21), it is assumed that $p \approx 7$, yielding the values of $\sigma \approx 1$ and $\gamma \approx 2/5$. In these approximations, the coefficient of the second term of the left-hand side in Eq. (21) is unity, while the third term becomes negligible. In the following section, the equation of flow over sinusoidal sand beds is applied, assuming a gradually varied bed slope, so that it can be approximately assumed that $\kappa(h) = \partial^2 h / \partial x^2$ and $\kappa(\eta) = \partial^2 \eta / \partial x^2$.

VI. FORMATION OF SAND WAVES

The basic Eqs. (17), (20), and (21) developed in the preceding section are now applied to investigate the formation of sand waves along a horizontal plane sand bed. When the flow Froude number exceeds a certain lower limit, erosion of sand bed begins, and by the process of erosion of the upstream faces and deposition of the eroded sediment on the downstream faces, dune wave appears to propagate downstream. With progressive increase in flow Froude number, the dunes eventually disappear becoming a plane bed at higher flow regime; but at still higher Froude numbers, the antidunes appear to travel in the upstream direction. This movement is accompanied by a rapid erosion of the downstream face and subsequent deposition on the following upstream face of the antidune. In these processes, the bed sand is transported as bed load as well as suspended load in the case of antidune propagation. The division of sediment transport in this manner is convenient for the purpose of analysis as a relatively small fraction of sand particles is transported in either mode intermittently. The total-load transport q_T (by volume) per unit time and width is thus given by

$$q_T = q_B + \int_h^\eta \bar{u} c \, dy, \tag{22}$$

where q_B is the bed-load transport rate and c is the concentration of sand suspension. The total load satisfies the Exner's sediment continuity equation. It is

$$\frac{\partial q_T}{\partial x} = -(1-\rho_0)\frac{\partial h}{\partial t} - \frac{\partial}{\partial t}\int_h^\eta c(x,y,t)dy = -(1-\rho_0)\frac{\partial h}{\partial t}$$
$$- \frac{\partial}{\partial t}[(\eta - h)C], \tag{23}$$

where ρ_0 is the porosity of bed sand and $C(x,t)$ is the depth-averaged concentration given by

$$C(x,t) = \frac{1}{\eta - h}\int_h^\eta c(x,y,t)dy. \tag{24}$$

Following the modification due to bed slope in the bed-load transport equation of Meyer-Peter and Müller [26], as was done by Fredsøe [13], the equation of bed-load transport q_B is given by

$$q_B = 8\sqrt{(s-1)gd^3}\left[\frac{\tau_0}{(s-1)\rho g d} - \mu\frac{\partial h}{\partial x} - 0.047\right]^{3/2}, \tag{25}$$

where s is the relative density of sand, d is the median sediment size, and μ is the particle frictional coefficient (of the

order of 0.1). The bed shear stress is obtained from the Manning equation of flow resistance as $\tau_0 = \rho g n^2 U^2 / (\eta - h)^{1/3}$. Consequently, the erosion of a sand bed is greater near the crest of the sand wave. The sediment concentration c in suspension satisfies the fluid-sediment continuity equation [1,13]. The equation is an advection-diffusion equation of the type

$$\frac{Dc}{Dt} = w_s \frac{\partial c}{\partial y} + \left(\varepsilon_x \frac{\partial^2 c}{\partial x^2} + \varepsilon_y \frac{\partial^2 c}{\partial y^2}\right), \tag{26}$$

where w_s is the terminal fall velocity of sand, ε_x is the turbulent diffusivity in x direction, and ε_y is the turbulent diffusivity in y direction. The diffusivities ε_x and ε_y are dependent on flow conditions. Thackston and Krenkel [27] estimated ε_x as

$$\varepsilon_x = 7.25 u_\tau D\left(\frac{U}{u_\tau}\right)^{1/4} = 7.25 g^{3/8} n^{3/4} U D^{7/8}. \tag{27}$$

On the other hand, Lane and Kalinske [28] estimated ε_y as

$$\varepsilon_y = \frac{1}{15}u_\tau D = 0.066 g^{1/2} n U D^{5/6}. \tag{28}$$

For the present analysis, from Eq. (23), the quantity of interest is the depth-averaged concentration C. Therefore, using Eq. (2) into Eq. (26) and integrating between limits h to η yields

$$\int_h^\eta \frac{Dc}{Dt}dy = \frac{\partial}{\partial t}[(\eta - h)C] + \frac{\partial}{\partial x}\int_h^\eta \bar{u}c \, dy. \tag{29}$$

In the flow domain, the time-averaged velocity $\bar{u}$ increases with height y, while c diminishes. Hence, in Eq. (29), it can be assumed that $\bar{u}c \approx UC$, replacing the velocity and the concentration by the averaged values. The integral of the right-hand side in Eq. (26) equals

$$\left(w_s c + \varepsilon_y \frac{\partial c}{\partial y}\right)_h^\eta + \varepsilon_x \int_h^\eta \frac{\partial^2 c}{\partial x^2}dy \approx \varepsilon_x \frac{\partial^2}{\partial x^2}[(\eta - h)C]. \tag{30}$$

In the above, the first term vanishes as there is no net vertical sediment flux across the extreme levels at $y = h$ and $y = \eta$ [1]. Equation (26) thus leads to

$$\frac{\partial}{\partial t}[(\eta - h)C] + \frac{\partial}{\partial x}[(\eta - h)UC] = \varepsilon_x \frac{\partial^2}{\partial x^2}[(\eta - h)C]. \tag{31}$$

It is important to point out that Eq. (31) is approximately legitimate. Thus, using Eqs. (22), (25), and (31) into the Exner equation, that is, Eq. (23), finally yields

$$(1-\rho_0)\frac{\partial h}{\partial t} + \varepsilon_x \frac{\partial^2}{\partial x^2}[(\eta - h)C] + 12[(s-1)gd^3]^{0.5}\left[\frac{n^2 U^2}{(\eta-h)^{1/3}(s-1)d} - \mu\frac{\partial h}{\partial x} - 0.047\right]^{0.5}$$
$$\times \left\{\frac{n^2}{(\eta-h)^{1/3}(s-1)d}\left[2U\frac{\partial U}{\partial x} - \frac{1}{3}\frac{U^2}{\eta-h}\left(\frac{\partial \eta}{\partial x} - \frac{\partial h}{\partial x}\right)\right]\right.$$
$$\left.- \mu\frac{\partial^2 h}{\partial x^2}\right\} = 0. \tag{32}$$

Equations (17) and (21) (with $\sigma = 1$ and $\gamma = 2/5$), (31) and (32) constitute the governing equation of perturbed flow due to erosion of bed. In Eq. (21), $\kappa(h) = \partial^2 h / \partial x^2$ and $\kappa(\eta) = \partial^2 \eta / \partial x^2$ are taken.

In analogy of propagation of waves along the interface of two immiscible liquids, the conditions for propagation of sand waves is investigated for a mean flow depth D and a mean flow velocity U_m over an undisturbed plane bed. The above set of equations to the first order is then linearized as

$$\frac{\partial \eta}{\partial t} - \frac{\partial h}{\partial t} + D\frac{\partial U}{\partial x} + U_m\left(\frac{\partial \eta}{\partial x} - \frac{\partial h}{\partial x}\right) = 0, \qquad (33a)$$

$$\frac{\partial U}{\partial t} + U_m\frac{\partial U}{\partial x} + \frac{2}{5}DU_m^2\left(\frac{\partial^3 \eta}{\partial x^3} + \frac{7}{16}\frac{\partial^3 h}{\partial x^3}\right) + g\frac{\partial \eta}{\partial x} + \frac{gn^2U_m^2}{D^3} = 0, \qquad (33b)$$

$$\frac{\partial C}{\partial t} + U_m\frac{\partial C}{\partial x} + C_0\frac{\partial U}{\partial x} = \varepsilon_x\frac{\partial^2 C}{\partial x^2}, \qquad (33c)$$

$$(1 - \rho_0)\frac{\partial h}{\partial t} + \varepsilon_x D\frac{\partial^2 C}{\partial x^2} + G\left\{\frac{n^2 U_m}{(s-1)dD^{1/3}}\left[2\frac{\partial U}{\partial x} - \frac{1}{3}\frac{U_m}{D}\left(\frac{\partial \eta}{\partial x} - \frac{\partial h}{\partial x}\right)\right] - \mu\frac{\partial^2 h}{\partial x^2}\right\} = 0, \qquad (33d)$$

where G is $12[n^2gd^2U_m^2D^{-1/3} - 0.047(s-1)gd^3]^{0.5}$ and C_0 is the initial average concentration that may occur due to mean flow velocity U_m. As was done by Engelund [13], if an exponential distribution of C_0 is assumed with ε_y given by Eq. (29), the average concentration C_0 is

$$C_0 = 4.853 \times 10^{-4}\frac{g^2n^4U_m^4}{w_s^4D^{2/3}}. \qquad (34)$$

Equations (33a)–(33d) with Eq. (34) form a system of linear differential equations. For propagating waves such as dunes and antidunes, the solution must be of the form

$$(\eta, h, U, C) = (\bar{E}, \bar{H}, \bar{U}, \bar{C})\exp(-\lambda t)\exp(ikx), \qquad (35)$$

where k is the wave number and λ is a complex number, whose imaginary part $\text{Im}(\lambda)$ and real part $\text{Re}(\lambda)$ represent circular frequency and exponential decay rate, respectively. The constants $\bar{E}$, $\bar{H}$, $\bar{U}$, and $\bar{C}$ are the complex constants involving amplitude and possible phase differences between two different components in Eq. (35). For an unstable bed resulting in a moving wavy bedform $h = \bar{H}\exp[-\text{Re}(\lambda)t]\exp\{i[kx - \text{Im}(\lambda)t]\}$ which grows with time $t > 0$ if $\text{Re}(\lambda) < 0$. The exponential growth with time is actually inhibited by the nonlinear nature of the parent flow Eqs. (17), (21), (31), and (32) that are lost in the linear instability analysis. Under unstable conditions, therefore, saturation of amplitude sets in resulting in wavy bedforms for all time. Thus, for unstable bedforms $\text{Re}(\lambda) < 0$ and for stable beds $\text{Re}(\lambda) > 0$. By substitution of Eq. (35), noting that the constant term (last term) in Eq. (33b) has no role in such an unstable solution analysis; the following linear algebraic equations are obtained:

$$(-\lambda + ikU_m)(\bar{E} - \bar{H}) + ikD\bar{U} = 0, \qquad (36a)$$

$$i\left(kg - \frac{2}{5}k^3DU_m^2\right)\bar{E} - \frac{7}{40}ik^3DU_m^2\bar{H} + (-\lambda + ikU_m)\bar{U} = 0, \qquad (36b)$$

$$ikC_0\bar{U} + (-\lambda + ikU_m + \varepsilon_x k^2)\bar{C} = 0, \qquad (36c)$$

$$-(1 - \rho_0)\lambda\bar{H} - \varepsilon_x Dk^2\bar{C} + G\left\{\frac{ikn^2U_m}{(s-1)dD^{4/3}}\left[2D\bar{U} - \frac{1}{3}U_m(\bar{E} - \bar{H})\right] + \mu k^2\bar{H}\right\} = 0. \qquad (36d)$$

Eliminating $\bar{E}$, $\bar{H}$, $\bar{U}$, and $\bar{C}$ from Eqs. (33a)–(33d), one obtains the quartic equation for λ:

$$(\lambda - ikU_m - \varepsilon_x k^2)\left\{\left[(1 - \rho_0)\frac{\lambda}{G} - \mu k^2\right]\left[(\lambda - ikU_m)^2 + k^2D\left(-\frac{2}{5}Dk^2U_m^2 + g\right)\right] + \frac{n^2k^2U_m}{(s-1)dD^{1/3}} \times \left(2\lambda - \frac{7}{3}ikU_m\right)\left(-\frac{23}{40}Dk^2U_m^2 + g\right)\right\} - \varepsilon_x\frac{k^4C_0D}{G}(\lambda - ikU_m)\left(-\frac{23}{40}Dk^2U_m^2 + g\right) = 0. \qquad (37)$$

Equation (37) has four complex roots. For the formation of sand waves, the real part of at least one root in Eq. (37) must be negative. If a root simultaneously possesses a positive real part, it represents a quickly decaying mode without altering overall instability. In terms of nondimensional quantities as $X = \lambda(D/g)^{0.5}$; $\beta = kD$, that is the wave number relative to mean flow depth; $F_m = U_m/(gD)^{0.5}$, that is, the Froude number; $\varphi_0 = D\varphi/[(s-1)d]$; $\varphi = n^2g/D^{1/3}$, that is, the bed characteristic parameter; $\varphi_A = 12(F_m^2\varphi_0 - 0.047)^{0.5}/[(s-1)(\varphi_0/\varphi)^{3/2}]$; $\varepsilon = \varepsilon_x/(gD^3)^{0.5} = 7.25\varphi^{3/8}F_m$; and $C_0 = 4.853 \times 10^{-4}(F_m^2/\varphi^2)(u_\tau/w_s)^4$, Eq. (37) can be written as a quartic equation of X. It is

$$(-X + i\beta F_m + \varepsilon\beta^2)\left\{\left[(1 - \rho_0)\frac{X}{\varphi_A} - \mu\beta^2\right]\left[(X - i\beta F_m)^2 + \beta^2\left(-\frac{2}{5}\beta^2F_m^2 + 1\right)\right] + \varphi_0\beta^2F_m\left(2X - \frac{7}{3}i\beta F_m\right) \times \left(-\frac{23}{40}\beta^2F_m^2 + 1\right)\right\} + \varepsilon\frac{C_0\beta^4}{\varphi_A}(X - i\beta F_m)\left(-\frac{23}{40}\beta^2F_m^2 + 1\right) = 0. \qquad (38)$$

Equation (38) is amenable to solution by the Muller method for specific numerical values of the parameters. Reasonable values of the different parameters are selected as $\rho_0 = 0.4$, $s = 2.65$, $\varphi = 2.5 \times 10^{-3}$, $\varphi_0 = 600\varphi$, and $u_\tau/w_s = 0.6$ for the computation of the four roots of X for different values of wave number β and Froude number F_m. It may be noted that
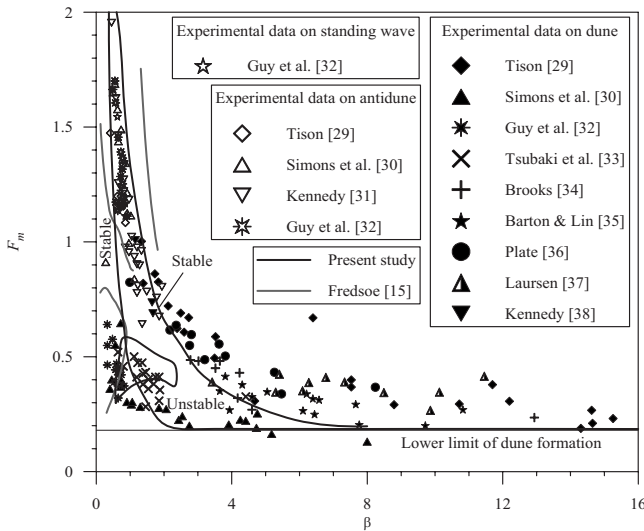
FIG. 2. Comparison of stability diagram obtained from present study with that of Fredsøe [15] and experimental data reported by various investigators.

any changed values of these parameters close to their reasonable values would not make any significant change in results. It transpires that there is at least one root with negative real part when the points (β, F_m) in the β-F_m plot, shown in Fig. 2, lie in a curved band forming a zone in which bedforms propagate with time. In fact, in this zone, there is one root with negative real part if $F_m > 0.8$; while there are two roots with negative real part if $F_m \leq 0.8$. To the left side of and below the left bounding curve, all the roots have either positive real part or do not exist at all, forming a stable zone. On the other hand, on the right bounding curve, the roots cease to exist indicating stability, and beyond for higher values of β, only one root possesses negative real part. The dispersion curves for most $-\mathrm{Re}(\lambda)$, expressed in nondimensional form as $-\mathrm{Re}(X)$ versus β, plotted in Fig. 3 for $F_m=0.3$, 0.5, 0.8, and 1, do not extend to the left of the bounding curve of the
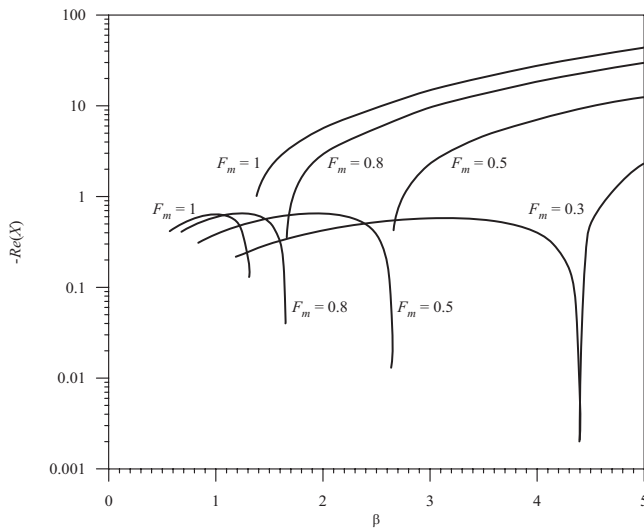

FIG. 3. Dispersion curves for $-\mathrm{Re}(\lambda)$ expressed in nondimensional form as $-\mathrm{Re}(X)$ versus β, for $F_m=0.3$, 0.5, 0.8, and 1.

unstable zone; while there is a discontinuity in dispersion curves along the right bounding curve of the unstable zone followed by steeply rising curves. However, the dispersion curves are convex upward. The crescent shaped unstable zone in Fig. 2, where significant sediment transport takes place as bed load and suspended load, contains the experimental data of antidunes and also of standing waves, having higher Froude numbers (greater than approximately 0.8), reported by various investigators [29–32]. The zone shrinks to an asymptotic critical line at $F_m=0.177$ when β becomes large. Below this theoretical value no root of Eq. (38) exists and bed erosion is inhibited due to significant reduction in flow velocity. If C_0 is set equal to zero, the transport phenomenon is due to bed load only. In this case, the boundary of the unstable zone degenerates into a small enclosed zone above $F_m=0.3$. The asymptotic line $F_m=0.177$ may be called the *lower limit for dune formation*. In fluvial hydraulics, the usual practice is that the sediment transport threshold is defined by the *Shields parameter*, $\Theta=\tau_0/[(s-1)\rho g d]$. The relationship $\Theta=\varphi_0 F_m^2$ produces the Shields parameter Θ equaling 0.047 corresponding to $F_m=0.177$ for the lower limit for dune formation. Thus, this model is applicable for the Froude number $F_m>0.177$ or the Shields parameter $\Theta>0.047$. For validation, experimental data of dunes are used because such moving bedforms appear at relatively low Froude numbers due to significant bed-load transport accompanied by a possible small suspended load. The available data are due to Tison [29], Simons *et al.* [30], Guy *et al.* [32], Tsubaki *et al.* [33], Brooks [34], Barton and Lin [35], Plate [36], Laursen [37], and Kennedy [38]. Importantly, a group of data of dunes, for low values of $\beta<3$, apparently lies in the enclosed inner zone, while another group of data with $\beta>3$ (approximately) appears to lie in the outer unstable zone following the critical limit line and becoming independent of the Froude number. There is a possible uncertainty that the data for $\beta>3$ may be for other features like ripples and not particularly for dunes (such as ripples superimposed on dunes) as there remains the difficulty of obtaining accurate data of dunes. However, in Fig. 2, it is evident that in the dune zone, the stability limits change considerably by the influence of gravity. This is in accordance with the fact that the bed-load transport is the principal sediment transport mechanism in the dunal regime, whereas the formation of antidune is significantly associated with the suspended load of sediment transport. This is in conformity with the present curves in general. However, the sand wave formation defined by the flow model is plausibly supported by the experimental data. There is also possible uncertainty associated with experimental scatter, as Fredsøe [15], who also used some of these experimental data for validation, pointed out the difficulty of obtaining accurate data on dunes that some data might be for other features such as ripples and ripples superimposed on dunes. In this context, it is important to mention that the present theory provides an estimation that is superior to Fredsøe's [15] theory that was unable to produce well-defined curves (which were rather fragmented) to separate out the stable and unstable zones (see Fig. 2) and did not provide the lower limit of dune formation. The basic difference between Fredsøe's [15] approach and present approach is that Fredsøe [15] applied vorticity transport equation to
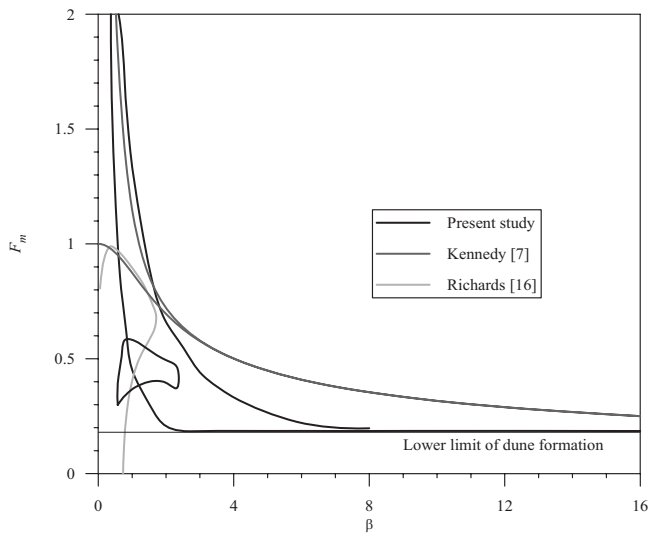
FIG. 4. Comparison of stability diagram obtained from present study with those of Kennedy [7] and Richards [16].

analyze stability of flow; while the present approach is based on integration of RANS equations. The gist of Fredsøe's [15] curves is that in the dune zone the stability limits change considerably by the effect of gravity. This is in conformity with the present curves in general. Figure 4 shows the comparison of the stability diagram obtained from present analysis with those of Kennedy [7] and Richards [16]. Using potential flow criterion, Kennedy [7] determined downstream migration of bed-forms from the conditions $F_m < (\tanh \beta / \beta)^{0.5}$ and $F_m > (\beta \tanh \beta)^{-0.5}$; while for upstream migration of bed-forms, the conditions are of opposite sense. However, his diagram does provide a sufficient unstable zone for subcritical response and the lower limit of dune formation. Experiments evidence that there remains considerable unstable zone for $F_m < 1$ (see Fig. 2). The reason is attributed to the fact that to study the instability, Kennedy [7] assumed a parameter that accounted for the lag of the local sediment transport rate behind the local velocity on the bed. There was a great uncertainty with the physical interpretation and evaluation of the lag parameter. On the other hand, Richards [16] provided stability limits to the formation of dunes. The stable dunes can exist in the zone facing the convex side of the curve; while dunes remain unstable on the other side of

the curve. A close observation of the data plots in Fig. 2 and the unstable zone of the curve given by Richards [16] shown in Fig. 4 that a large number of data of stable dune lie within the unstable zone. Moreover, he did not provide any information on the lower limit of dune formation.

VII. CONCLUSIONS

A theory of turbulent shear flow over an undulating sand bed has been evolved to deal with the instability principle of plane sand beds in free-surface flows leading to the formation of sand waves. The theory is based on the RANS equations and the time-averaged continuity equation. For analysis, the time-averaged streamwise velocity and the bed resistance are assumed to follow the $1/p$th power law ($p \approx 7$) and the Manning equation, respectively. Two basic equations obtained, in this way, have been given by Eqs. (17) and (20) or Eq. (21), which can be regarded as the generalized Saint Venant equations.

In instability of a horizontal plane sand-bed in free-surface flows, the curves of the Froude number versus nondimensional wave number of bedforms define an instability zone for bedforms due to erosion by combined bed-load and suspended-load transports. At higher Froude numbers (greater than approximately 0.8), the bedforms remain unstable as standing waves and antidunes because the experimental data fall within the instability zone. At lower Froude numbers, if suspended-load transport is neglected, the instability zone is reduced to a small closed zone above Froude number exceeding 0.3. A number of data plots of dunes belong to this zone although some data of dunes remain scattered. The two instability zones lie above the lower limit for dune formation, where the Froude number is 0.177. Nevertheless, the formation of sand waves obtained from the flow model is reasonably supported by the experimental data.

[1] W. H. Graf, *Hydraulics of Sediment Transport* (McGraw-Hill, New York, 1971).

[2] F. Engelund and J. Fredsøe, Annu. Rev. Fluid Mech. **14**, 13 (1982).

[3] A. J. Raudkivi, *Loose Boundary Hydraulics* (Balkama, Rotterdam, 1998).

[4] N. Chien and Z. Wan, *Mechanics of SedimentTransport* (ASCE Press, Virginia, 1999).

[5] A. G. Anderson, in Proceedings of the Third Mid-Western Conference on Fluid Mechanics (University of Minnesota,

Minneapolis, 1953), p. 379.

[6] T. B. Benjamin, J. Fluid Mech. **6**, 161 (1959).

[7] J. F. Kennedy, J. Fluid Mech. **16**, 521 (1963).

[8] F. M. Exner, Sitzungsber. Akad. Wiss. Wien, Math.-Naturwiss. Kl., Abt. 2A **134**, 165 (1925).

[9] A. J. Reynolds, J. Fluid Mech. **22**, 113 (1965).

[10] F. Engelund and J. Fredsøe, Nord. Hydrol. **2**, 93 (1971).

[11] F. Engelund and E. Hansen, Acta Polytechnica Scandinavica, Series 3 (1966), .

[12] T. Hayashi, J. Hydr. Div. **96**, 357 (1970).

[13] F. Engelund, J. Fluid Mech. **42**, 225 (1970).

[14] J. D. Smith, J. Geophys. Res. **75**, 5928 (1970).

[15] J. Fredsøe, J. Fluid Mech. **64**, 1 (1974).

[16] K. J. Richards, J. Fluid Mech. **99**, 597 (1980).

[17] C. C. S. Song, J. Hydr. Eng. **109**, 1133 (1983).

[18] S. Onda and T. Hosoda, J. Hydrosci. Hydr. Eng. **23**, 13 (2005).

[19] H. Nakagawa and T. Tsujimoto, J. Hydraul. Eng. **110**, 467 (1984).

[20] W. C. Kuru, D. T. Leighton, and M. J. McCready, Int. J. Multiphase Flow **21**, 1123 (1995).

[21] S. E. Coleman, J. J. Fedele, and M. H. Garcia, J. Hydraul. Eng. **129**, 956 (2003).

[22] H. Schlichting, *Boundary Layer Theory* (McGraw-Hill, New York, 1968).

[23] S. Dey, Proc. R. Soc. London, Ser. A **458**, 283 (2002).

[24] S. K. Bose and S. Dey, Proc. R. Soc. London, Ser. A **463**, 369 (2007).

[25] S. K. Bose and S. Dey, J. Hydraul. Eng. **133**, 1074 (2007).

[26] E. Meyer-Peter and R. Müller, in *Proceedings of the Second Meeting of the International Association for Hydraulic Research, Stockholm, Sweden* (IAHR, Delft, The Netherlands, 1948), Vol. 3, p. 39.

[27] E. L. Thackston and P. A. Krenkel, J. Sanit. Engrg. Div. **93**, 67 (1967).

[28] E. W. Lane and A. A. Kalinske, Trans., Am. Geophys. Union **20**, 603 (1941).

[29] L. H. Tison, in Transactions of the Third Meeting of the International Association for Hydraulic Structures Research, Grenoble, France, 1949 (unpublished).

[30] D. B. Simons, E. V. Richardson, and M. L. Albertson, Geol. Survey Wat. Supply Paper No. 1498-A (U.S. GPO, Washington, D.C., 1961).

[31] J. F. Kennedy, M. Keck Laboratory of Hydraulics and Water Resources, California Institute of Technology Report No. KH-R-2, W, 1961 (unpublished).

[32] H. P. Guy, D. B. Simons, and E. V. Richardson, U.S. Geol. Surv. Prof. Pap. **462-I**, 1 (1966).

[33] T. Tsubaki, T. Kawasumi, and T. Yasutomi, Rep. Res. Inst. Appl. Mech. (Kyushu Univ.) **2**, 241 (1953).

[34] N. H. Brooks, Doctoral thesis, California Institute of Technology, 1954.

[35] J. R. Barton and P. N. Lin, Colorado A. and M. College Report No. 55JRB2, 1955 (unpublished).

[36] E. J. O. F. Plate, Master thesis, Colorado State University, 1957.

[37] E. M. Laursen, J. Hydr. Div. **84**, 1 (1958).

[38] J. F. Kennedy, M. Keck Laboratory of Hydraulics and Water Resources, California Institute of Technology Report No. KH-R-3, W, 1961 (unpublished).